IEEE Access
Multidisciplinary | Rapid Review | Open Access Journal

SPECIAL SECTION ON ADVANCED MODELING AND CONTROL OF COMPLEX MECHATRONIC SYSTEMS WITH NONLINEARITY AND UNCERTAINTY

Received August 4, 2018, accepted August 16, 2018, date of publication August 21, 2018, date of current version September 7, 2018.

Digital Object Identifier 10.1109/ACCESS.2018.2866270

Continuous Integral Robust Control of Electro-Hydraulic Systems With Modeling Uncertainties

WUNING MA, WENXIANG DENG, AND JIANYONG YAO

School of Mechanical Engineering, Nanjing University of Science and Technology, Nanjing 210094, China

Corresponding author: Jianyong Yao (jerryyao.buaa@gmail.com)

This work was supported in part by the National Natural Science Foundation of China under Grant 51675279, in part by the Natural Science Foundation of Jiangsu Province under Grant BK20170035, and in part by the Fundamental Research Funds for the Central Universities under Grant 309171A8801.

ABSTRACT This paper studies the high-performance tracking control of electro-hydraulic systems with consideration of both mismatched and matched modeling uncertainties. A continuous integral robust control strategy is proposed based on the backstepping design framework. By introducing a novel error transformation, the mismatched modeling uncertainty can be transmitted to the control input channel, and then, the constructed integral robust structure in the proposed controller can handle it together with the matched modeling uncertainty. The acceleration signal that usually suffers heavy noise contamination is not required in the controller, and the final control input is continuously differentiable, which is benefit for tracking performance improvement and practical controller implementation. The closed-loop system stability is analyzed via the Lyapunov theory, and it reveals that the proposed controller achieves an asymptotic tracking performance with zero steady-state error in the presence of various modeling uncertainties. Comparative experiments are performed to demonstrate the effectiveness of the proposed control strategy.

INDEX TERMS Electro-hydraulic system, modeling uncertainty, integral robust control, asymptotic tracking.

I. INTRODUCTION

Electro-hydraulic systems have been extensively employed in modern industry since they have small size-to-power ratios and large torque/force output capabilities [1]. However, high-performance control design for electro-hydraulic systems has always been a challenging issue since the dynamics of hydraulic systems are highly nonlinear. Moreover, hydraulic systems are typically subjected to various modeling uncertainties which can be classified as parametric uncertainties (e.g., uncertain viscous friction coefficient and effective oil bulk modulus) and uncertain nonlinearities (e.g., unmodeled nonlinear friction effects and external disturbances) [2], [3]. Therefore, developing high-performance control strategy for electro-hydraulic systems with various modeling uncertainties has attracted wide attention.

To deal with the parametric uncertainties in electro-hydraulic systems, numerous of adaptive controllers have been developed, such as [4]–[7]. However, performance degradation may be caused in these adaptive controllers when facing large unmodeled disturbances. Sliding mode control methods have also been developed to attenuate various modeling uncertainties for electro-hydraulic systems due to their strong robustness [8], [9]. However, the chattering caused by the control action of sliding mode control might excite the neglected high-frequency dynamics and result in system instability. Although some modifications can be made to the traditional sliding mode control to avoid control chattering, such as using saturation function to replace the discontinuous signum function [10], the excellent asymptotic stability result will be lost. In [3], an adaptive robust control (ARC) approach was proposed by Yao for tracking control of an asymmetric hydraulic cylinder, which aims to cope with the parametric uncertainties and uncertain nonlinearities together. Unlike the traditional adaptive control, a projection type adaptive law was synthesized which can ensure the parameter estimations are always bounded and then a deterministic nonlinear robust control law was synthesized to ensure prescribed transient and steady-state tracking performance. Adaptive

robust control has also been widely applied to lots of other practical plants, such as linear motors [11], [12], active suspensions [13], [14], and industrial biaxial gantries [15], [16]. In addition, some other control approaches have been developed by using various disturbance observers to estimate the modeling uncertainties and then to achieve performance improvement, such as extended state observer based control [17], high-gain disturbance observer based control [18], and time delay estimation based control [19], [20].

It can be noted that all abovementioned control schemes can only ensure the trajectory tracking error to be bounded when considering both parametric uncertainties and uncertain nonlinearities. To obtain excellent asymptotic tracking performance with a continuous control law, a nonlinear robust control strategy called the robust integral of the sign of the error (RISE) was proposed in [21]. It has been successfully employed to cope with the tracking control problem of motor servo systems [22], [23] quadrotor unmanned aerial vehicle (UAV) [24], helicopter [25], as well as friction identification issue of Euler-Lagrange system [26]. Some adaptive version RISE control schemes have also been researched to reduce the control effort and achieve tracking performance improvement. For instance, desired-trajectory-based adaptive RISE controllers were designed for electromechanical servo system [27] and hydraulic system [28] modeled in a chain of integrators form. In [29], adaptive RISE control based on immersion and invariance (I&I) concept was studied for tracking control of a quadrotor UAV. However, all these RISE-based control methods were only applicable for systems with matched modeling uncertainties, i.e., the uncertainties appear in the control input channel. Generally, practical electro-hydraulic systems have both mismatched and matched uncertainties. The so-called mismatched uncertainties refer to those uncertainties entering the system through different channels from that of the control input. In [30], by using an experimental internal leakage model to precisely describe the leakage characteristics, the modeling errors of the pressure dynamics were neglected and a RISE-based adaptive controller was proposed to achieve high-accuracy tracking for hydraulic systems. The RISE feedback term was utilized to accommodate for the smooth mismatched modeling uncertainties and adaptive laws were synthesized to handle the matched parametric uncertainties. It is worth noting that the acceleration signal which usually suffers heavy measurement noise was required in the controller in [30] and the final control input is discontinuous due to the differentiation operation of the RISE feedback law, which may lead to degraded tracking performance. Though a modified signum function was used to approximate the standard signum function in the experiment, the rigor of the theoretical proof was destroyed and asymptotic tracking performance will no longer be guaranteed.

In this paper, a high-performance-oriented continuous integral robust controller is proposed for an electro-hydraulic system with both mismatched and matched modeling uncertainties. Based on the backstepping design framework, the mismatched uncertainties can be transmitted to the control input channel and handled together with the matched uncertainties by a novel integral robust structure. Due to the separation of the derivative of the virtual control law, the heavy noise-contaminated acceleration signal is not used in the designed controller. In addition, the final control input is continuously differentiable, which indicates control chattering can be avoided and improved tracking performance will be obtained. The proposed continuous integral robust controller theoretically guarantees an asymptotic tracking performance with zero steady-state tracking error, which is vital for high-performance tracking control of practical electro-hydraulic systems. The high-performance nature of the proposed control strategy is demonstrated by comparing it with the other four existing control approaches in the experiments.

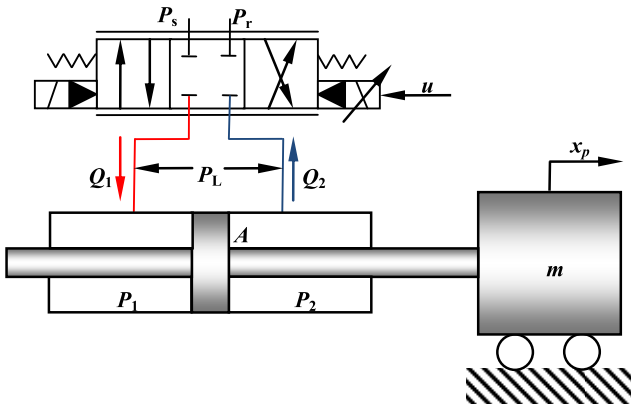

FIGURE 1. The schematic diagram of electro-hydraulic system.

The remaining of this paper is structured as follows. Section II shows the nonlinear mathematical model of the electro-hydraulic system. The detailed design of the proposed continuous integral robust controller and its main theoretical results are presented in Section III. Experimental validation results are obtained in Section IV. Section V gives the conclusions of this paper.

II. NONLINEAR MODEL OF ELECTRO-HYDRAULIC SYSTEM

The schematic diagram of the studied electro-hydraulic system is shown in Fig. 1. The dynamics equation of the load can be given by

$$m\ddot{x}_p = (P_1 - P_2)A - F_f(\dot{x}_p) + F_d(t) \tag{1}$$

where m is the total mass of the piston and the load; x_p is the displacement of the load; $P_L = P_1 - P_2$ denotes the load pressure, in which P_1 and P_2 are pressures of the forward chamber and return chamber, respectively; A is the pressure area of the piston; F_f represents the modeled nonlinear frictions; and F_d denotes the mismatched modeling uncertainty including unmodeled frictions, parameter deviations, etc.

The flow continuity equations of the two chambers can be given by [1], [30]

$$\begin{aligned}\frac{V_1}{\beta_e}\dot{P}_1 &= -A\dot{x}_p - C_t P_L + q_{e1}(t) + Q_1\\ \frac{V_2}{\beta_e}\dot{P}_2 &= A\dot{x}_p + C_t P_L - q_{e2}(t) - Q_2\end{aligned} \tag{2}$$

where $V_1 = V_{01} A x_p$, $V_2 = V_{02} - A x_p$ are the control volumes of the cylinder chambers, in which V_{01} and V_{02} are the initial control volumes; β_e is the effective oil bulk modulus; C_t is the internal leakage coefficient of the cylinder; $q_{e1}(t)$ and $q_{e2}(t)$ are modeling errors caused by leakage characteristics and unmodeled valve effects such as valve dead-zone [33]; Q_1 is the supplied flow rate to the forward chamber, and Q_2 is the return flow rate of the return chamber. The flow equation of the valve for Q_1 and Q_2 can be given by [1], [30]:

$$\begin{aligned}Q_1 &= k_q x_v[s(x_v)\sqrt{P_s - P_1} + s(-x_v)\sqrt{P_1 - P_r}]\\ Q_2 &= k_q x_v[s(x_v)\sqrt{P_2 - P_r} + s(-x_v)\sqrt{P_s - P_2}]\end{aligned} \tag{3}$$

where $k_q = C_d w\sqrt{2/\rho}$ is the flow gain of the valve; P_s is the supply pressure and P_r is the return pressure of the fluid; and

$$s(x_v) = \begin{cases}1, & \text{if } x_v \geq 0\\ 0, & \text{if } x_v < 0\end{cases} \tag{4}$$

Noting that the servo valve used in the studied hydraulic system is of high-response, the valve dynamics can be ignored which means it can be approximated as a proportional element, i.e, $x_v = k_i u$, where x_v is the spool position, u is the control input voltage applied to the servo valve, and k_i is a positive electrical gain. Hence, the flow equation of the valve can be rewritten as

$$\begin{aligned}Q_1 &= k_t u[s(u)\sqrt{P_s - P_1} + s(-u)\sqrt{P_1 - P_r}]\\ Q_2 &= k_t u[s(u)\sqrt{P_2 - P_r} + s(-u)\sqrt{P_s - P_2}]\end{aligned} \tag{5}$$

where $k_t = k_q k_i$ is the total flow gain.

III. CONTINUOUS INTEGRAL ROBUST CONTROLLER DESIGN

A. DESIGN MODEL AND ISSUES TO BE ADDRESSED

There are lots of friction models to describe the complex nonlinear friction effects, such as modified LuGre model [4] and continuously differentiable static friction model [31]. However, to reflect the strong robustness of the proposed control strategy against modeling uncertainties, the modeled friction term F_f is simply considered as viscous friction in this paper, i.e., $F_f = B\dot{x}_p$, in which B is the viscous friction coefficient, other unmodeled frictions such as Coulomb friction and Stribeck effect are lumped into the modeling uncertainty term F_d. In addition, since the physical parameters of the hydraulic system such as B, β_e, C_t can be identified offline in practical applications, their nominal values are utilized in the control design and the deviations between the nominal and true values are also treated as modeling uncertainties.

Define the state variables as $x = [x_1, x_2, x_3]^{\mathrm{T}} = [x_p, \dot{x}_p, AP_L/m]^{\mathrm{T}}$, thus the electro-hydraulic system can be expressed in a state space form as

$$\begin{aligned}\dot{x}_1 &= x_2\\ \dot{x}_2 &= x_3 - bx_2 + D(t)\\ \dot{x}_3 &= g_1(u, x_3)u - g_2(x_2) - g_3(x_3) + Q(t)\end{aligned} \tag{6}$$

where $b = B/m$, $D(t) = F_d/m$, $g_2(x_2) = \beta_e A^2(1/V_1 + 1/V_2)x_2/m$, $g_3(x_3) = \beta_e C_t(1/V_1 + 1/V_2)x_3$, $Q(t) = \beta_e A(q_{e1}/V_1 + q_{e2}/V_2)/m$, and $g_1(u, x_3) = A\beta_e k_t(\chi_1/V_1 + \chi_2/V_2)/m$, in which

$$\begin{aligned}\chi_1 &= s(u)\sqrt{P_s - P_1} + s(-u)\sqrt{P_1 - P_r}\\ \chi_2 &= s(u)\sqrt{P_2 - P_r} + s(-u)\sqrt{P_s - P_2}\end{aligned} \tag{7}$$

The goal is to synthesize a continuous control input u such that the position of the load x_1 can track any motion trajectory $x_{1d}(t)$ as closely as possible in the presence of both mismatched modeling uncertainty $D(t)$ and matched modeling uncertainty $Q(t)$. Before the controller design, the following assumptions are made.

Assumption 1: The desired motion trajectory $x_{1d}(t)$ is bounded and continuously differentiable up to third order; the studied hydraulic system is working under normal conditions such that the following property is satisfied, i.e., $0 < P_{\mathrm{r}} < P_1 < P_{\mathrm{s}}$, $0 < P_{\mathrm{r}} < P_2 < P_{\mathrm{s}}$ [4], [5].

Assumption 2: The modeling uncertainties $D(t)$ and $Q(t)$ are smooth enough and bounded such that the following defined new disturbance $\Delta(t)$ has bounded time derivatives up to third order, i.e.,

$$|\dot{\Delta}(t)| \leq \delta_1, \quad |\ddot{\Delta}(t)| \leq \delta_2, \ |\Delta(t)| \leq \delta_3 \tag{8}$$

where δ_1, δ_2 and δ_3 are known positive constants, and

$$\Delta(t) = \dot{D}(t) + (k_3 - \frac{\partial \alpha_2}{\partial x_2})D(t) + Q(t) \tag{9}$$

in which $k_3 > 0$ and α_2 are control gain and virtual control law, respectively. The specific expression of α_2 will be given subsequently.

Remark 1: The assumption that P_1 and P_2 are bounded by P_{r} and P_{s} is very common in hydraulic control area. Based on this assumption, it is obviously that the state $x_3 = AP_L/m$ is naturally bounded. Since $1/(s + b)$ is a stable transfer function, it can be inferred from the second equation of (6) that x_2 is also bounded, and then the boundedness of $\dot{x}_2$ can also be concluded. This specific property of electro-hydraulic system will be used in the stability analysis.

B. CONTROLLER DESIGN

The proposed continuous integral robust controller design parallels the backstepping design procedure [32] due to the mismatched modeling uncertainty. The detailed control design procedure is given as follows.

Step 1: Let a set of error variables be defined as

$$z_2 = \dot{z}_1 + k_1 z_1 = x_2 - \alpha_1, \quad \alpha_1 = \dot{x}_{1d} - k_1 z_1$$
$$z_3 = x_3 - \alpha_2 \tag{10}$$

where $z_1 = x_1 - x_{1\mathrm{d}}(t)$ is the position tracking error; $k_1 > 0$ is a feedback gain to be tuned; α_1 is the virtual control function for x_2; α_2 is the virtual control function for x_3 which will be synthesized later.

Noting (6) and (10), the time derivative of z_2 can be given by

$$\begin{aligned}\dot{z}_2 &= \dot{x}_2 - \dot{\alpha}_1 \\ &= z_3 + \alpha_2 - bx_2 + D(t) - \dot{\alpha}_1\end{aligned} \tag{11}$$

Based on (11), the virtual control function α_2 can be designed as

$$\alpha_2 = bx_2 + \dot{\alpha}_1 - k_2 z_2 \tag{12}$$

where $k_2 > 0$ is a feedback gain to be tuned.

Substituting (12) into (11) yields

$$\dot{z}_2 = z_3 - k_2 z_2 + D(t) \tag{13}$$

Step 2: Noting (6) and (10), the time derivative of z_3 can be shown as

$$\begin{aligned}\dot{z}_3 &= \dot{x}_3 - \dot{\alpha}_2 \\ &= g_1(u, x_3)u - g_2(x_2) - g_3(x_3) + Q(t) - \dot{\alpha}_2\end{aligned} \tag{14}$$

Since $\dot{\alpha}_2$ has unknown part due to the mismatched uncertainty $D(t)$, it is grouped into the following two parts

$$\begin{aligned}\dot{\alpha}_2(t, x_1, x_2) &= \dot{\alpha}_{2c} + \dot{\alpha}_{2u}, \\ \dot{\alpha}_{2c} &= \frac{\partial \alpha_2}{\partial t} + \frac{\partial \alpha_2}{\partial x_1} x_2 + \frac{\partial \alpha_2}{\partial x_2}(x_3 - bx_2), \\ \dot{\alpha}_{2u} &= \frac{\partial \alpha_2}{\partial x_2} D(t).\end{aligned} \tag{15}$$

where $\dot{\alpha}_{2c}$ denotes the part of $\dot{\alpha}_2$ with known information and can be used for feedforward compensation, $\dot{\alpha}_{2u}$ is the unknown part because of the mismatched modeling uncertainty.

Hence, based on (14) and (15), the final continuous integral robust control law is synthesized as

$$\begin{aligned}u &= u_a + u_s, \quad u_s = u_{s1} + u_{s2}, \\ u_a &= \frac{1}{g_1}(g_2 + g_3 + \dot{\alpha}_{2c}), \\ u_{s1} &= -\frac{1}{g_1} k_3 z_3\end{aligned} \tag{16}$$

where k_3 is a positive feedback control gain, u_a is the model-based feedforward compensation term to achieve tracking performance improvement, and u_s is the robust control law in which u_{s1} is a linear feedback term to stabilize the nominal hydraulic system and u_{s2} is a nonlinear robust term to overcome the modeling uncertainty.

Applying the designed control input (16) to (14), the dynamic of z_3 can be given by

$$\dot{z}_3 = -k_3 z_3 + g_1 u_{s2} - \frac{\partial \alpha_2}{\partial x_2} D(t) + Q(t) \tag{17}$$

To handle the modeling uncertainty, the nonlinear robust control law u_{s2} is designed as the following integral robust structure

$$u_{s2} = -\frac{1}{g_1}\{k_r z_2 - k_r z_2(0) + \int_0^t [k_r k_2 z_2 + \beta sign(z_2)]\mathrm{d}\tau\} \tag{18}$$

where k_r and β are positive control gains, sign (z_2) is the standard signum function with respect to z_2.

Remark 2: With the separation in (15), the final control input does not use the acceleration signal $\dot{x}_2$ which is accompanied by heavy measurement noise. In addition, the proposed control law (16) is continuous. However, the acceleration signal is needed in the RISE control design in [30], and the final control input is discontinuous due to the signum function. Hence, in comparison to the controller in [30], the proposed continuous integral robust controller is more suitable for practical implementation and improved tracking performance can be expected.

C. MAIN RESULTS

Similar to [34], we introduce a new error variable as

$$\varsigma = z_3 + D(t) \tag{19}$$

where ς is an auxiliary signal to help the stability analysis, and not utilized in control. From (13), it can be inferred that if the controller (16) can make ς go to 0, then z_2 and z_1 will go to 0.

Noting (17) and (18), we have

$$\begin{aligned}\dot{\varsigma} &= \dot{z}_3 + \dot{D}(t) \\ &= -k_3 z_3 - k_r z_2 + k_r z_2(0) - \int_0^t [k_r k_2 z_2 + \beta sign(z_2)]\mathrm{d}\tau \\ &\quad - \frac{\partial \alpha_2}{\partial x_2} D(t) + Q(t) + \dot{D}(t) \\ &= -k_3 \varsigma - k_r z_2 + k_r z_2(0) \\ &\quad - \int_0^t [k_r k_2 z_2 + \beta sign(z_2)]\mathrm{d}\tau + \Delta(t)\end{aligned} \tag{20}$$

It can be known from (13) that

$$\dot{z}_2 = -k_2 z_2 + \varsigma \tag{21}$$

Using (21), (20) can be further written as

$$\dot{\varsigma} = -k_3 \varsigma - \int_0^t [k_r \varsigma + \beta sign(z_2)]\mathrm{d}\tau + \Delta(t) \tag{22}$$

Define an auxiliary variable Ψ as

$$\Psi = \Delta(t) - \int_0^t [k_r \varsigma + \beta sign(z_2)]\mathrm{d}\tau \tag{23}$$

then (22) can be rewritten as

$$\dot{\varsigma} = -k_3 \varsigma + \Psi \tag{24}$$

The following lemma is first introduced since it will be invoked in the stability analysis.

Lemma 1: Let an auxiliary function $L(t)$ be defined as

$$L(t) = \frac{1}{k_3 k_r}\Psi[\dot{\Delta}(t) - \beta sign(z_2)] \tag{25}$$

If the tuned gain β satisfying the following condition:

$$\beta \geq \delta_1 + \frac{\delta_3 + (k_2 + k_3)\delta_2}{k_2 k_3} \tag{26}$$

then the following function $R(t)$ is always positive,

$$R(t) = R(0) - \int_0^t L(\tau)\mathrm{d}\tau \tag{27}$$

where

$$R(0) = \frac{2}{k_3 k_r}\max\{|\dot{z}_2|(\delta_1 + \beta) + |z_2|[\delta_2 + (k_2 + k_3)(\delta_1 + \beta)]\} \tag{28}$$

Proof: See Appendix A.

Theorem 1: If the gain β is selected to satisfy the condition (26) and the feedback gains k_1, k_2 and k_3 are chosen large enough such that the matrix Λ defined below is positive definite

$$\Lambda = \begin{bmatrix} k_1 & -\frac{1}{2} & 0 \\ -\frac{1}{2} & k_2 & -\frac{1}{2} \\ 0 & -\frac{1}{2} & k_3 \end{bmatrix} \tag{29}$$

then all the closed-loop system signals can be guaranteed to be bounded by the proposed continuous integral robust controller (16), and asymptotic output tracking can also be achieved, i.e., $z_1 \to 0$ as $t \to \infty$.

Proof: See Appendix B.

Remark 3: The theoretical results in Theorem 1 indicate that asymptotic output tracking performance can be obtained for electro-hydraulic systems in the presence of both mismatched and matched modeling uncertainties with the proposed continuous integral robust controller. It is of great significance for achieving high-performance tracking control of electro-hydraulic systems since various modeling uncertainties seriously restricts the high-performance control design.

IV. EXPERIMENTAL VALIDATION

A. EXPERIMENTAL SETUP

To test the above controller design, an experimental platform has been set up whose photograph is presented in Fig. 2. It consists of a bench case with a guide rail, a symmetric hydraulic cylinder, a linear encoder (Heidenhain LC483), two pressure sensors (MEAS US175-C00002-200BG), a high bandwidth servo valve (Moog G761-3003, rated flow is 19 L/min at 70 bar drop), a driving shaft, a mass load etc., a hydraulic supply and a measurement and control system. The measurement and control system consists of monitoring software and real time control software whose A/D card is Advantech PCI-1716, D/A card is Advantech PCI-1723,

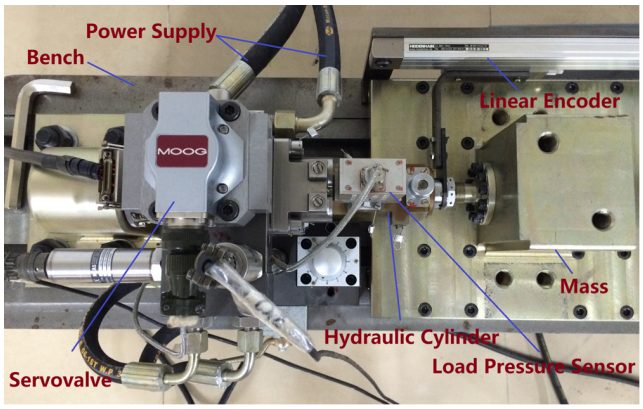

FIGURE 2. Experimental platform of electro-hydraulic system.

TABLE 1. Physical parameters of electro-hydraulic system.

Parameter	Value	Parameter	Value
m	30kg	k_t	1.1969×10^{-8}m^3/s/V/Pa$^{-1/2}$
A	904.778mm^2	V_{01}	3.98×10^{-5}m^3
B	4000N·s/m	V_{02}	3.98×10^{-5}m^3
C_t	1×10^{-12}m^3/s/Pa	P_s	10MPa
β_e	700MPa	P_r	0Pa

and Counter card is Heidenhain IK-220, all these cards are 16-bits. The sampling frequency is 2 kHz. More details about this platform can be found in [33]. The physical hydraulic parameters used in the experiment are given in Table I.

B. COMPARATIVE EXPERIMENTAL RESULTS

In the experiment, the continuous integral robust controller proposed in this paper is compared with other four controllers to illustrate its effectiveness and superiority more clearly. The compared controllers and their control gains are given as follows.

1) CIRC: The continuous integral robust controller proposed in this paper. The control gains are: $k_1 = 1800$, $k_2 = 600$, $k_3 = 100$, $k_r = 1000$, $\beta = 80000$.

2) FLC: The feedback linearization controller. The FLC does not have the nonlinear robust term in CIRC, it just has pure linear feedback term. The control gains of FLC are chosen as the same with those of CIRC.

3) RFC: The linear robust feedback controller without any model compensation. The effectiveness of model-based control design can be verified by comparing this controller with the others. Its control gains are also the same with CIRC.

4) PI: The widely used proportional-integral controller in industry. The P-gain and I-gain are tuned as $k_p = 8000$, $k_i = 2000$.

5) VFPI: The proportional-integral controller with velocity feedforward action which is also extensively used in industry. The VFPI controller can be expressed as

$$u_{\mathrm{VFPI}} = k_p z_1 + k_i \int z_1 \mathrm{d}t + k_f \dot{x}_{1d} \tag{30}$$

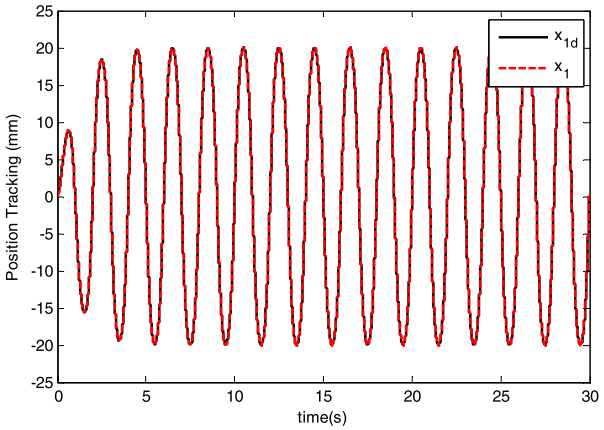

FIGURE 3. Position tracking of CIRC for 20mm-0.5Hz sinusoidal motion.

where k_p, k_i, k_f are P-gain, I-gain and velocity feedforward gain, respectively. The velocity feedforward gain $k_f = 28\text{V}\cdot\text{s/m}$ is determined via the open loop identification. k_p and k_i are selected to be the same with PI controller.

Additionally, three performance indices, i.e., the maximum, average, and standard deviation of the tracking errors, are utilized to assess the tracking performance of the above five controllers. The specific definitions of the performance indices are as follows [33].

1) Maximal absolute value of the tracking errors is defined as

$$M_E = \max_{i=1,\ldots,N}\{|z_1(i)|\} \tag{31}$$

where N is the number of the recorded digital signals, and is used as an index of measure of tracking accuracy.

2) Average tracking error is defined as

$$\mu = \frac{1}{N}\sum_{i=1}^{N}|z_1(i)| \tag{32}$$

and is used as an objective numerical measure of average tracking performance.

3) Standard deviation performance index is defined as

$$\sigma = \sqrt{\frac{1}{N}\sum_{i=1}^{N}[|z_1(i)| - \mu]^2} \tag{33}$$

to measure the deviation level of tracking errors.

The compared five controllers are first applied to a normal-level sinusoidal trajectory $x_{1\text{d}} = 20\text{actan}(\sin\pi t)[1\text{-exp}(\text{-}t)]/0.7854$ mm. The experimental results are obtained as shown in Fig. 3 $\sim$ Fig. 5. The steady-state performance indices are also presented in Table II. As shown in Fig. 3, the position of the load can well track the desired motion trajectory with the proposed CIRC controller. The performance indices in Table II and the comparative tracking errors in Fig. 4 reveal that the proposed CIRC achieves the best tracking performance. Specifically, since CIRC controller

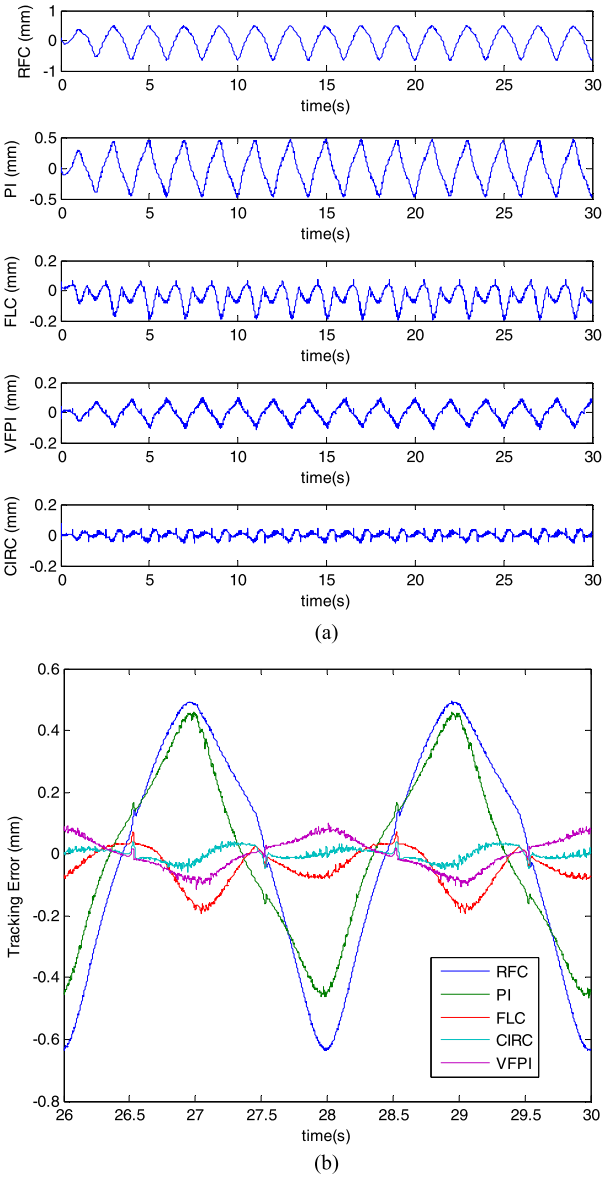

FIGURE 4. Comparative tracking errors for 20mm-0.5Hz sinusoidal motion. (a) Tracking errors of the five controllers during the whole time history. (b) Tracking errors of the five controllers during the last two cycles.

has nonlinear robust law to deal with the modeling uncertainties (mainly the unmodeled frictions), it obtains much better performance than FLC. It can be found that VFPI also obtains better tracking performance than FLC, the reason can be found by comparing RFC and PI. Since both RFC and PI are pure robust feedback controllers, the worse tracking performance of RFC in comparison to PI indicates that the robust gains of RFC are weaker than those of PI in some sense. Therefore, it can be understood that VFPI outperforms FLC, because it uses larger feedback gains and also has some model compensation as done in FLC. However, the tracking performance of VFPI is still worse than the proposed CIRC which uses the same feedback gains with RFC. The

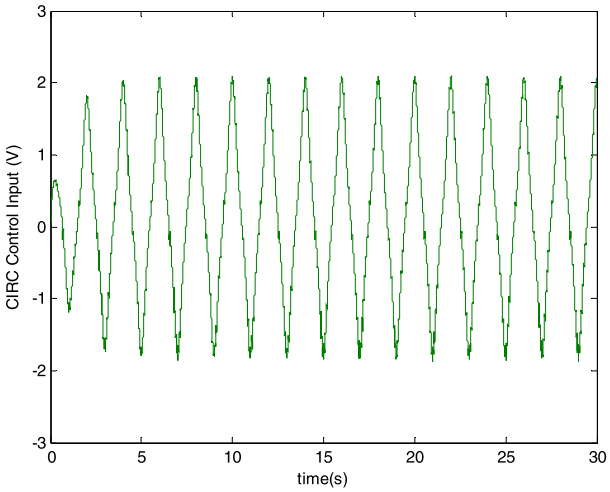

FIGURE 5. Control input of CIRC for 20mm-0.5Hz sinusoidal motion.

TABLE 2. Performance indices during the last two cycles for 20mm-0.5Hz sinusoidal motion.

Indices (mm)	M_E	μ	σ
RFC	0.6356	0.3120	0.1744
PI	0.4667	0.2362	0.1394
FLC	0.1942	0.0584	0.0483
VFPI	0.1122	0.0481	0.0269
CIRC	0.0582	0.0169	0.0114

TABLE 3. Performance indices during the last two cycles for 20mm-1Hz sinusoidal motion.

Indices (mm)	M_E	μ	σ
RFC	1.4281	0.6152	0.3890
PI	1.1132	0.4958	0.3299
FLC	0.4634	0.1438	0.1126
VFPI	0.2465	0.0725	0.0534
CIRC	0.1969	0.0625	0.0382

maximum tracking error of VFPI is nearly twice that of CIRC. By comparing the tracking errors of RFC and FLC, the advantages of model-based compensation design can be verified. The control input of CIRC is given in Fig. 5. As seen, it is continuous and bounded.

To further test the fast tracking performance of the compared controllers, the motion trajectory $x_{1d} = 20\text{actan}(\sin 2\pi t)[1\text{-exp}(\text{-}t)]/0.7854$ mm is utilized. The steady-state performance indices are presented in Table III. Position tracking of CIRC and comparative tracking errors are shown in Fig. 6 and Fig. 7, respectively. It can be seen that the proposed CIRC also outperforms the other four controllers in terms of all performance indices in this fast

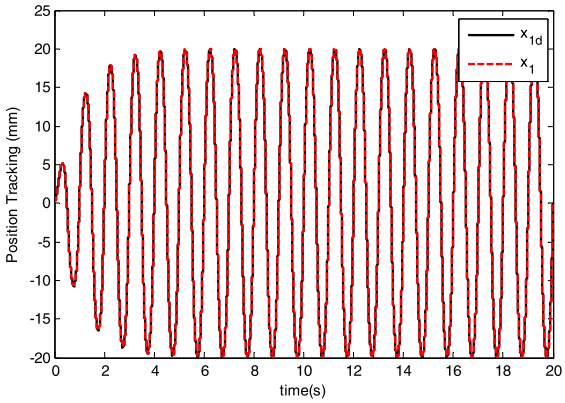

FIGURE 6. Position tracking of CIRC for 20mm-1Hz sinusoidal motion.

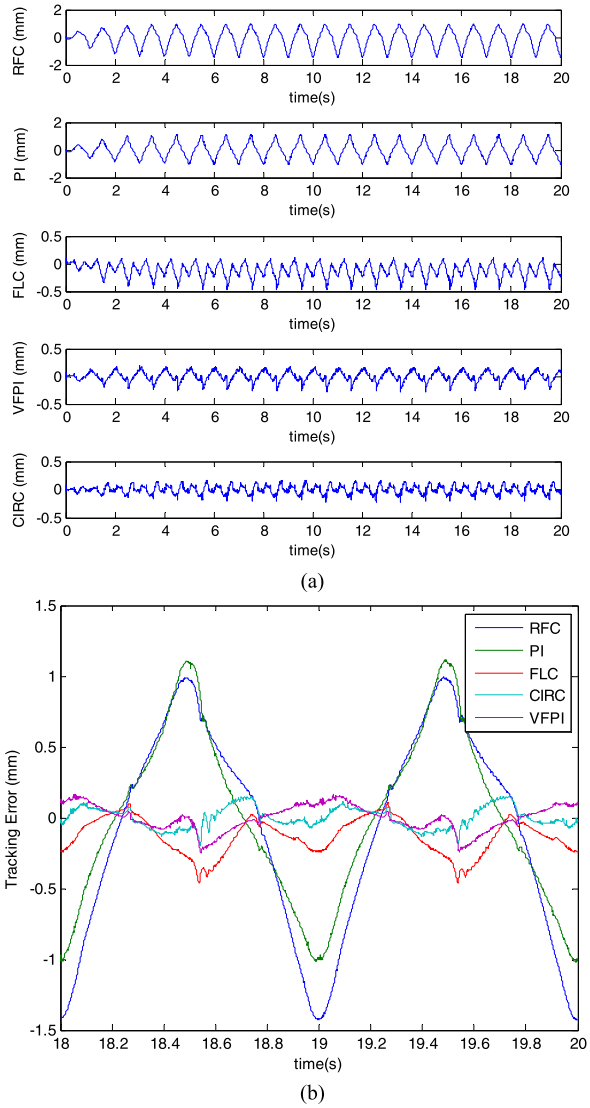

FIGURE 7. Comparative tracking errors for 20mm-1Hz sinusoidal motion. (a) Tracking errors of the five controllers during the whole time history. (b) Tracking errors of the five controllers during the last two cycles.

motion case. It can be found from Fig. 4 and Fig. 7 that the tracking error bias phenomenon happens to FLC due to the lack of nonlinear robust control law to overcome

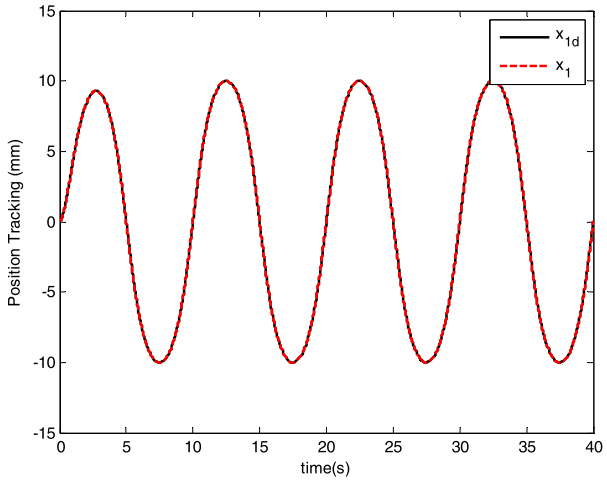

FIGURE 8. Position tracking of CIRC for 10mm-0.1Hz sinusoidal motion.

TABLE 4. Performance indices during the last cycle for 10mm-0.1Hz sinusoidal motion.

Indices (mm)	M_E	μ	σ
RFC	0.1434	0.0660	0.0467
PI	0.0241	0.0155	0.0053
FLC	0.0513	0.0348	0.0105
VFPI	0.0096	0.0028	0.0017
CIRC	0.0084	0.0006	0.0008

the effects of modeling uncertainties. This is more apparent in the subsequent slow motion case. The control input of CIRC is also regular and bounded, hence it is omitted here.

At last, a slow motion trajectory $x_{1d} = 10\text{actan}(\sin 0.2\pi t)\times[1\text{-exp}(\text{-}t)]/0.7854$ mm is utilized to further test the robustness of the proposed CIRC control strategy, since the nonlinear friction characteristics are mainly Stribeck effect in the low-velocity region which will cause degraded tracking performance in this case. Similarly, the experimental results are obtained and presented in Table IV, Fig. 8, and Fig. 9. As seen from the position tracking of CIRC in Fig. 8 and its tracking error in Fig. 9, it also achieves high-accuracy tracking in such slow motion case, which verifies its strong robustness against various modeling uncertainties. In comparison to the other four controllers, the proposed CIRC obtains both better transient and steady-state tracking performance. Though the maximum tracking error of CIRC is only a bit smaller than that of VFPI, its other two performance indices μ and σ are much smaller than those of VFPI, which reveals the high-performance nature of CIRC. Due to the effect of the Stribeck effect in this slow motion case and FLC only uses linear feedback law, its tracking error has more apparent bias than those of the former two cases. This further demonstrates the strong robustness of the proposed CIRC controller.

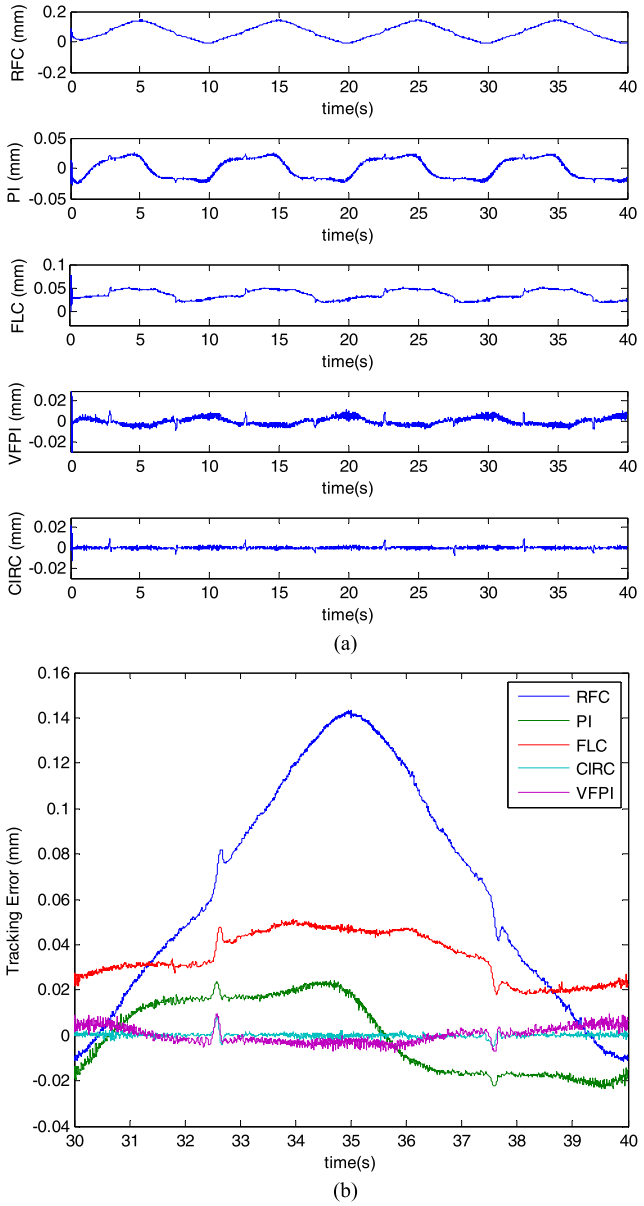

FIGURE 9. Comparative tracking errors for 10mm-0.1Hz sinusoidal motion. (a) Tracking errors of the five controllers during the whole time history. (b) Tracking errors of the five controllers during the last two cycles.

V. CONCLUSION

In this paper, a continuous integral robust controller is proposed for high-performance tracking control of an electro-hydraulic system via backstepping method. A significant outcome of the proposed controller is that mismatched and matched modeling uncertainties can be handled together in one controller and asymptotic output tracking performance is guaranteed with a continuous control input. Due to the separation of the differential of the virtual control function in the backstepping design procedure, the heavy noise-contaminated acceleration signal is not required in the proposed controller. Therefore, tracking performance

improvement will be obtained by the proposed control strategy and it is easier to be implemented in practice. It is theoretically proved by Lyapunov-based stability analysis that globally asymptotic tracking performance with zero steady-state tracking error can be achieved by the proposed controller. The proposed continuous integral robust controller was implemented on a valve-controlled double-rod hydraulic cylinder servo system and compared with four other controllers. Experimental results have verified its high performance nature.

APPENDIX A

Proof of Lemma 1: Noting (21) and (24), the auxiliary variable Ψ can also be expressed by

$$\begin{aligned}\Psi &= \dot{\varsigma} + k_3\varsigma \\ &= \ddot{z}_2 + (k_2+k_3)\dot{z}_2 + k_2k_3z_2 \end{aligned} \tag{A1}$$

Substituting (A1) into (25), and then integrating in time, we obtain

$$\begin{aligned}&\int_0^t L(\tau)\mathrm{d}\tau \\ &= \frac{1}{k_3k_r}\int_0^t [\ddot{z}_2 + (k_2+k_3)\dot{z}_2 + k_2k_3z_2][\dot{\Delta} - \beta\mathrm{sign}(z_2)]\mathrm{d}\tau \\ &= \frac{1}{k_3k_r}\int_0^t \ddot{z}_2\dot{\Delta}\mathrm{d}\tau + \frac{1}{k_3k_r}\int_0^t (k_2+k_3)\dot{z}_2\dot{\Delta}\mathrm{d}\tau \\ &\quad - \frac{\beta}{k_3k_r}\int_0^t \ddot{z}_2\mathrm{sign}(z_2)\mathrm{d}\tau - \frac{\beta}{k_3k_r}\int_0^t (k_2+k_3)\dot{z}_2\mathrm{sign}(z_2)\mathrm{d}\tau \\ &\quad + \int_0^t \frac{k_2}{k_r}z_2[\dot{\Delta} - \beta\mathrm{sign}(z_2)]\mathrm{d}\tau \end{aligned} \tag{A2}$$

Integrating the integrals on the right-hand side of (A2) by parts yields

$$\begin{aligned}&\int_0^t L(\tau)\mathrm{d}\tau \\ &= \frac{1}{k_3k_r}(\dot{z}_2\dot{\Delta}|_0^t - z_2\ddot{\Delta}|_0^t + \int_0^t z_2\Delta\mathrm{d}\tau) + \frac{k_2+k_3}{k_3k_r}(z_2\dot{\Delta}|_0^t \\ &\quad - \int_0^t z_2\ddot{\Delta}\mathrm{d}\tau) - \frac{\beta}{k_3k_r}\dot{z}_2\mathrm{sign}(z_2)|_0^t - \frac{(k_2+k_3)\beta}{k_3k_r}|z_2||_0^t \\ &\quad + \int_0^t \frac{k_2}{k_r}z_2[\dot{\Delta} - \beta\mathrm{sign}(z_2)]\mathrm{d}\tau \\ &= \frac{1}{k_3k_r}[\dot{z}_2\dot{\Delta} - \dot{z}_2(0)\dot{\Delta}(0) - z_2\ddot{\Delta} + z_2(0)\ddot{\Delta}(0)] \\ &\quad + \frac{k_2+k_3}{k_3k_r}[z_2\dot{\Delta} - z_2(0)\dot{\Delta}(0)] - \frac{\beta}{k_3k_r}[\dot{z}_2\mathrm{sign}(z_2) \\ &\quad - \dot{z}_2(0)\mathrm{sign}(z_2(0))] - \frac{(k_2+k_3)\beta}{k_3k_r}[|z_2| - |z_2(0)|] \\ &\quad + \int_0^t \frac{k_2}{k_r}z_2[\dot{\Delta} + \frac{\Delta - (k_2+k_3)\ddot{\Delta}}{k_2k_3} - \beta\mathrm{sign}(z_2)]\mathrm{d}\tau \end{aligned} \tag{A3}$$

The above equation can be upper bounded as

$$\begin{aligned}&\int_0^t L(\tau)\mathrm{d}\tau \\ &\le |\dot{z}_2|\frac{1}{k_3k_r}(|\dot{\Delta}| + \beta) + |z_2|[\frac{1}{k_3k_r}|\ddot{\Delta}| + \frac{k_2+k_3}{k_3k_r}(|\dot{\Delta}| + \beta)] \\ &\quad + |\dot{z}_2(0)|\frac{1}{k_3k_r}(|\dot{\Delta}(0)| + \beta) + |z_2(0)|[\frac{1}{k_3k_r}|\ddot{\Delta}(0)| \\ &\quad + \frac{k_2+k_3}{k_3k_r}(|\dot{\Delta}(0)| + \beta)] \\ &\quad + \int_0^t \frac{k_2}{k_r}|z_2|[|\dot{\Delta}| + \frac{|\Delta| + (k_2+k_3)|\ddot{\Delta}|}{k_2k_3} - \beta]\mathrm{d}\tau \end{aligned} \tag{A4}$$

Using assumption 2 and the sufficient condition in (26), it can be inferred from (A4) that the function $R(t)$ defined in (27) is always positive.

APPENDIX B

Proof of Theorem 1: Defining a Lyapunov function as

$$V(t) = \frac{1}{2}z_1^2 + \frac{1}{2}z_2^2 + \frac{1}{2k_3}\varsigma^2 + \frac{1}{2k_3k_r}\Psi^2 + R \tag{B1}$$

Noting (10), (13), (24) and (27), the time derivative of $V(t)$ can be given by

$$\begin{aligned}\dot{V} &= z_1\dot{z}_1 + z_2\dot{z}_2 + \frac{1}{k_3}\varsigma\dot{\varsigma} + \frac{1}{k_3k_r}\Psi\dot{\Psi} + \dot{R} \\ &= z_1(z_2 - k_1z_1) + z_2(\varsigma - k_2z_2) + \frac{1}{k_3}\varsigma(-k_3\varsigma + \Psi) \\ &\quad + \frac{1}{k_3k_r}\Psi[\dot{\Delta} - k_r\varsigma - \beta\mathrm{sign}(z_2)] \\ &\quad - \frac{1}{k_3k_r}\Psi[\dot{\Delta} - \beta\mathrm{sign}(z_2)] \\ &= -k_1z_1^2 + z_1z_2 - k_2z_2^2 + z_2\varsigma - k_3\varsigma^2 = -z^T\Lambda z \end{aligned} \tag{B2}$$

where $z = [z_1, z_2, \varsigma]^{\mathrm{T}}$. Since the matrix Λ can be ensured to be positive definite by tuning the control gains, the above equation can be further written as

$$\dot{V} \le -\lambda_{\min}(\Lambda)(z_1^2 + z_2^2 + \varsigma^2) \triangleq -\Xi \tag{B3}$$

where $\lambda_{\min}(\Lambda)$ is the minimal eigenvalue of matrix Λ. Hence, $V \in L_\infty$ and $\Xi \in L_2$, the signal z_1, z_2, ς are bounded. Then, the system states x_1, x_2, and x_3 can be inferred to be bounded based on assumption 1. Hence, the control input u is also bounded. Noting the expressions of the dynamics of z_1, z_2 and ς, the boundedness of the time derivative of the function Ξ can also be concluded, which indicates Ξ is a uniformly continuous function. According to Barbalat's lemma [32], it can be inferred that $\Xi \to 0$ as $t \to \infty$. This further leads to the results in *Theorem 1*.

ACKNOWLEDGMENT

The authors are very grateful to the help from Dr. D. X. Ba and his team to extend their results to this paper.

REFERENCES

[1] H. E. Merritt, *Hydraulic Control Systems*. New York, NY, USA: Wiley, 1967.

[2] C. Guan and S. Pan, "Nonlinear adaptive robust control of single-rod electro-hydraulic actuator with unknown nonlinear parameters," *IEEE Trans. Control Syst. Technol.*, vol. 16, no. 3, pp. 434–445, May 2008.

[3] B. Yao, F. Bu, J. Reedy, and G. T.-C. Chiu, "Adaptive robust motion control of single-rod hydraulic actuators: Theory and experiments," *IEEE/ASME Trans. Mechatronics*, vol. 5, no. 1, pp. 79–91, Mar. 2000.

[4] J. Yao, W. Deng, and Z. Jiao, "Adaptive control of hydraulic actuators with LuGre model-based friction compensation," *IEEE Trans. Ind. Electron.*, vol. 62, no. 10, pp. 6469–6477, Oct. 2015.

[5] J. Yao, Z. Jiao, and D. Ma, "A practical nonlinear adaptive control of hydraulic servomechanisms with periodic-like disturbances," *IEEE/ASME Trans. Mechatronics*, vol. 20, no. 6, pp. 2752–2760, Dec. 2015.

[6] Q. Guo, J. Yin, T. Yu, and D. Jiang, "Saturated adaptive control of an electrohydraulic actuator with parametric uncertainty and load disturbance," *IEEE Trans. Ind. Electron.*, vol. 64, no. 10, pp. 7930–7941, Oct. 2017.

[7] G. Shen, X. Li, Z. Zhu, Y. Tang, and W. Zhu, "Acceleration tracking control combining adaptive control and off-line compensators for six-degree-of-freedom electro-hydraulic shaking tables," *ISA Trans.*, vol. 70, pp. 322–337, Sep. 2017.

[8] T.-T. Chen and Y.-Y. Wu, "An optimal variable structure control with integral compensation for electrohydraulic position servo control systems," *IEEE Trans. Ind. Electron.*, vol. 39, no. 5, pp. 460–463, Oct. 1992.

[9] S. Ik Han and J. M. Lee, "Adaptive dynamic surface control with sliding mode control and RWNN for robust positioning of a linear motion stage," *Mechatronics*, vol. 22, no. 2, pp. 222–238, 2012.

[10] M. R. A. Atia, S. A. Haggag, and A. M. M. Kamal, "Enhanced electromechanical brake-by-wire system using sliding mode controller," *J. Dyn. Syst., Meas., Control*, vol. 138, no. 4, p. 041003, 2016.

[11] Z. Chen, B. Yao, and Q. Wang, "Accurate motion control of linear motors with adaptive robust compensation of nonlinear electromagnetic field effect," *IEEE/ASME Trans. Mechatronics*, vol. 18, no. 3, pp. 1122–1129, Jun. 2013.

[12] Z. Chen, B. Yao, and Q. Wang, "μ-synthesis-based adaptive robust control of linear motor driven stages with high-frequency dynamics: A case study," *IEEE/ASME Trans. Mechatronics*, vol. 20, no. 3, pp. 1482–1490, Jun. 2015.

[13] W. Sun, H. Gao, and O. Kaynak, "Vibration isolation for active suspensions with performance constraints and actuator saturation," *IEEE/ASME Trans. Mechatronics*, vol. 20, no. 2, pp. 675–683, Apr. 2015.

[14] W. Sun, Z. Zhao, and H. Gao, "Saturated adaptive robust control for active suspension systems," *IEEE Trans. Ind. Electron.*, vol. 60, no. 9, pp. 3889–3896, Sep. 2013.

[15] M. Yuan, Z. Chen, B. Yao, and X. Zhu, "Time optimal contouring control of industrial biaxial gantry: A highly efficient analytical solution of trajectory planning," *IEEE/ASME Trans. Mechatronics*, vol. 22, no. 1, pp. 247–257, Feb. 2017.

[16] M. Yuan, Z. Chen, B. Yao, and J. Hu, "An improved on-line trajectory planner with stability-guaranteed critical test curve algorithm for generalized parametric constraints," *IEEE/ASME Trans. Mechatronics*, to be published, doi: 10.1109/TMECH.2018.2862144.

[17] J. Yao and W. Deng, "Active disturbance rejection adaptive control of hydraulic servo systems," *IEEE Trans. Ind. Electron.*, vol. 64, no. 10, pp. 8023–8032, Oct. 2017.

[18] D. Won, W. Kim, D. Shin, and C. C. Chung, "High-gain disturbance observer-based backstepping control with output tracking error constraint for electro-hydraulic systems," *IEEE Trans. Control Syst. Technol.*, vol. 23, no. 2, pp. 787–795, Mar. 2015.

[19] Y. Wang, L. Gu, Y. Xu, and X. Cao, "Practical tracking control of robot manipulators with continuous fractional-order nonsingular terminal sliding mode," *IEEE Trans. Ind. Electron.*, vol. 63, no. 10, pp. 6194–6204, Oct. 2016.

[20] Y. Wang, F. Yan, S. Jiang, and B. Chen, "Time delay control of cable-driven manipulators with adaptive fractional-order nonsingular terminal sliding mode," *Adv. Eng. Softw.*, vol. 121, pp. 13–25, Jul. 2018.

[21] B. Xian, D. M. Dawson, M. S. D. Queiroz, and J. Chen, "A continuous asymptotic tracking control strategy for uncertain nonlinear systems," *IEEE Trans. Autom. Control*, vol. 49, no. 7, pp. 1206–1211, Jul. 2004.

[22] J. Yao, Z. Jiao, and D. Ma, "RISE-based precision motion control of DC motors with continuous friction compensation," *IEEE Trans. Ind. Electron.*, vol. 61, no. 12, pp. 7067–7075, Dec. 2014.

[23] S. Wang, J. Na, and X. Ren, "RISE-based asymptotic prescribed performance tracking control of nonlinear servo mechanisms," *IEEE Trans. Syst., Man, Cybern. Syst.*, to be published, doi: 10.1109/TSMC.2017.2769683.

[24] B. Xian, C. Diao, B. Zhao, and Y. Zhang, "Nonlinear robust output feedback tracking control of a quadrotor UAV using quaternion representation," *Nonlinear Dyn.*, vol. 79, no. 4, pp. 2735–2752, 2015.

[25] Z. Li, H. H. T. Liu, B. Zhu, H. Gao, and O. Kaynak, "Nonlinear robust attitude tracking control of a table-mount experimental helicopter using output feedback," *IEEE Trans. Ind. Electron.*, vol. 62, no. 9, pp. 5665–5676, Sep. 2015.

[26] C. Makkar, G. Hu, W. G. Sawyer, and W. E. Dixon, "Lyapunov-based tracking control in the presence of uncertain nonlinear parameterizable friction," *IEEE Trans. Autom. Control*, vol. 52, no. 10, pp. 1988–1994, Oct. 2007.

[27] W. Deng and J. Yao, "Adaptive integral robust control and application to electromechanical servo systems," *ISA Trans.*, vol. 67, pp. 256–265, Mar. 2017.

[28] J. Yao, W. Deng, and Z. Jiao, "RISE-based adaptive control of hydraulic systems with asymptotic tracking," *IEEE Trans. Autom. Sci. Eng.*, vol. 14, no. 3, pp. 1524–1531, Jul. 2017.

[29] B. Zhao, B. Xian, Y. Zhang, and X. Zhang, "Nonlinear robust adaptive tracking control of a quadrotor UAV via immersion and invariance methodology," *IEEE Trans. Ind. Electron.*, vol. 62, no. 5, pp. 2891–2902, May 2015.

[30] J. Yao, Z. Jiao, D. Ma, and L. Yan, "High-accuracy tracking control of hydraulic rotary actuators with modeling uncertainties," *IEEE/ASME Trans. Mechatronics*, vol. 19, no. 2, pp. 633–641, Apr. 2014.

[31] C. Makkar, W. E. Dixon, W. G. Sawyer, and G. Hu, "A new continuously differentiable friction model for control systems design," in *Proc. IEEE/ASME Int. Conf. Adv. Intell. Mechatron.*, Jul. 2005, pp. 600–605.

[32] M. Krstic, I. Kanellakopoulos, and P. V. Kokotovic, *Nonlinear and Adaptive Control Design*. New York, NY, USA: Wiley, 1995.

[33] W. Deng, J. Yao, and D. Ma, "Robust adaptive precision motion control of hydraulic actuators with valve dead-zone compensation," *ISA Trans.*, vol. 70, pp. 269–278, Sep. 2017.

[34] X. B. Dang, H. Yeom, J. Kim, and J. Bae, "Gain-adaptive robust backstepping position control of a BLDC motor system," *IEEE/ASME Trans. Mechatronics*, to be published, doi: 10.1109/TMECH.2018.2864187.

WUNING MA received the B.Tech. degree from Suzhou University, Suzhou, China, in 2003, and the Ph.D. degree in mechatronics from the Nanjing University of Science and Technology, Nanjing, China, 2016.

In 2016, he joined the School of Mechanical Engineering, Nanjing University of Science and Technology, where he is currently a Lecturer. His current research interests include servo control of mechatronic systems and structure dynamics analysis.

WENXIANG DENG received the B.Tech. degree in mechanical engineering from Central South University, Changsha, China, in 2013. He is currently pursuing the Ph.D. degree with the School of Mechanical Engineering, Nanjing University of Science and Technology, Nanjing, China.

His current research interests include servo control of mechatronic systems, robust adaptive control, and nonlinear compensation.

JIANYONG YAO received the B.Tech. degree from Tianjin University, Tianjin, China, in 2006, and the Ph.D. degree in mechatronics from the Beihang University, Beijing, China, in 2012. He was a Visiting Exchange Student with the School of Mechanical Engineering, Purdue University, from 2010 to 2011.

In 2012, he joined the School of Mechanical Engineering, Nanjing University of Science and Technology, Nanjing, China, where he is currently a Full Professor. His current research interests include servo control of mechatronic systems, adaptive and robust control, fault detection, and accommodation of dynamic systems.